Avalanche dynamics of the continuous damage fiber bundle model

R. C. Hidalgo
AMADE, Departament de Física, Departament de Enginyeria Mecànica i de la Construcciò Industrial, Universitat de Girona Av. Montilivi s/n, 17071-Girona, Spain

F. Kun
Department of Theoretical Physics, University of Debrecen, P.O.Box: 5, H-4010 Debrecen, Hungary

K. Kovács
Department of Appl. Math. and Prob. Theory, University of Debrecen,P.O.Box: 5, H-4010 Debrecen, Hungary

Ignacio Pagonabarraga
Departament de Física Fonamental, Universitat de Barcelona
Carrer Martí i Franqués, 1, 08028-Barcelona, Spain
(Dated: April 23, 2009)

We present a detailed analytical and numerical study of the avalanche statistics of the continuous damage fiber bundle model. In the model, linearly elastic fibers undergo a series of partial failure events which give rise to a gradual degradation of their stiffness. Varying the two parameters of the model, i.e. the maximum number of local failures and the degree of stiffness reduction in single events, the model provides various types of material responses with experimental relevance. We show by analytic calculations that the presence of plasticity and hardening in the macroscopic constitutive behavior results in power law distributed breaking bursts with a spectrum of exponents. We derive the phase diagram of the model system, which provides an overview of all possible burst distributions. Our results generalize previous analytical findings and bring a new unified view of the statistics of breaking avalanches in fiber bundles models.

PACS numbers: 46.50.+a, 05.20. Dd

I. INTRODUCTION

The damage and fracture of heterogeneous materials is a very interesting scientific problems with a broad spectrum of technological applications [1–3]. It is well known that under a constant or slowly increasing external load, the fracture of heterogeneous materials proceeds in bursts, i.e. local breakings occur in correlated avalanches separated by silent periods [4–13]. Since the bursting activity generates elastic waves, it can be recorded by means of the acoustic emission technique being the primary source of information on the microscopic dynamics of fracture. Recently, experiments on a large variety of materials with disordered micro-structure pointed out that the amplitude and energy distributions of acoustic signals, furthermore, the waiting times in between, are characterized by power laws, where the exponents show a certain degree of universality [4–13].

Among the theoretical approaches to the problem, the fiber bundle model (FBM) plays a crucial role, since it captures the main ingredients of the fracture of disordered materials but it is still simple enough to facilitate analytical calculations [14–28]. In FBM the specimen is discretized in terms of parallel fibers which are subject to a longitudinal external load. The fibers have identical elastic properties but stochastically distributed breaking thresholds. Quasi-statically increasing the external load to break a single fiber, an entire avalanche of fiber breakings can be triggered due to the redistribution of load over the remaining intact fibers. It has been shown in the framework of FBM that in the limit of equal load sharing the size distribution of bursts follows a power law behavior with an exponent 5/2 universal for a broad class of disorder distributions [15–20]. It was shown analytically that when bursts are recorded solely in the vicinity of the critical point of macroscopic failure a crossover occurs to a lower value of the exponent 3/2. The crossover of the bursts size exponent when approaching the critical point addresses the possibility to design techniques to forecast the imminent failure event [20, 23].

For theoretical studies on the statistical aspects of fracture, it is a great challenge to understand the origin of the scale free bursting activity, to reveal the role of the underlying disorder and of the breaking mechanisms, and to explore the possible universality classes [19, 20, 25–28]. Recently, we have shown by analytical and numerical means that mixing fibers of strongly different strength, i.e. when the bundle is composed of two subsets of fibers, where one subset is unbreakable, the avalanche size distribution exhibits a transition from the well known exponent 5/2 to a lower one 9/4 when the mixing ratio surpasses a threshold value [21].

In the present paper we investigate the effect of the breaking mechanism of fibers on the statistics of avalanches based on the continuous damage fiber bundle model (CDFBM) introduced recently [29–31]. In CDFBM the fibers do not suffer instantaneous failure when the local load exceeds their breaking threshold, instead they loose their stiffness gradually in a sequence of partial breaking events. The gradual breaking sequence is characterized by two parameters: the fraction of stiffness kept by the fiber after a partial breaking, and the total number of allowed breakings. Varying the two parameters, the model provides various types of mechanical responses from simple quasi-brittle behavior through plasticity to hardening. We demonstrate by analytical calculations that depending on the details of the constitutive curve, the size distribution of bursts has a power law functional form with a spectrum of exponents between 2.5 and 2.0. We construct the phase diagram of the model which provides an overview of all possible avalanche behaviors. The analytical calculations are verified by computer simulations, furthermore, the results are compared to recent experimental findings.

II. CONTINUOUS DAMAGE FIBER BUNDLE MODEL

The continuous damage fiber bundle model was introduced recently [29–31] as an extension of the classical fiber bundle model [14, 16]. The model consists of a set of N linearly elastic fibers with identical Young modulus E_f organized into a parallel bundle. Under an increasing external load the fibers exhibit brittle failure, i.e. they have a linearly elastic behavior up to a critical load σ_{th} where they break. The fibers have an identical Young modulus E_f, however, the breaking threshold σ_{th} is a stochastic variable characterized by a probability density $p(\sigma_{th})$ and a distribution function $P(\sigma_{th})$. The fiber bundle is loaded uniaxially giving rise to a global deformation f, which is related to the applied load through $\sigma = E_f f$. In the classical FBM, when fiber i experiences a local load σ_i larger than its strength threshold, σ_{th}^i, it fails so that its stiffness is set to zero.

As a novel element, in CDFBM it is assumed that the failure of fibers is not instantaneous, instead the fibers undergo a gradual degradation process. When the local load of fiber i reaches its breaking threshold σ_{th}^i it suffers only partial failure such that its stiffness E_f is reduced by a factor $0 \leq \alpha \leq 1$. When the external load is further increased the fiber again exhibits a linear elastic behavior but with a lower value of the Young modulus αE_f, and hence, it can fail again in the same manner as before. The maximum number of breaking events k_{max} the fibers can suffer together with the stiffness reduction factor α are very important parameters of CDFBM. It is important to note that once a fiber has failed it can either keep the same strength threshold, which corresponds to a quenched distribution of failure strengths, or choose a different strength value from the prescribed threshold distribution, corresponding to an annealed distribution of failure strengths. It has been presented in Refs. [29–31] that depending on the way how the stiffness of fibers is treated after k_{max} number of failure events, the model can describe both macroscopic hardening and

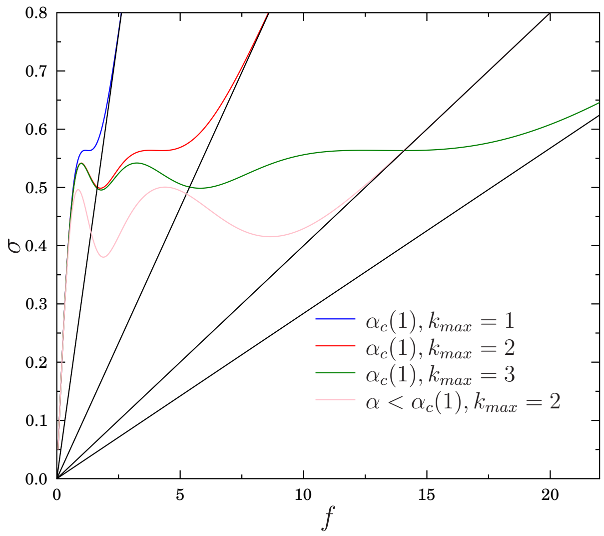

FIG. 1: *(Color online)* Constitutive behavior of the continuous damage fiber bundle model for a fixed value of the stiffness reduction parameter $\alpha = \alpha_c(k_{max} = 1)$ varying the number of allowed failures k_{max}.

macroscopic fracture of the bundle. Hardening behavior is obtained when the fibers retain their $\alpha^{k_{max}} E_f$ stiffness after having failed k_{max} times. In this case the macroscopic constitutive equation of the system converges to an asymptotic linear behavior. Setting the stiffness of fibers to zero after k_{max} breakings implies the complete failure of the fibers which then leads to macroscopic fracture of the entire bundle instead of hardening. In the present paper our study is restricted to the case of quenched disorder and macroscopic hardening in the final state.

When the fibers are allowed to break only once $k_{max} = 1$, the constitutive equation of the fiber bundle can simply be obtained as

$$\sigma = \frac{F}{N} = f(1 - P(f)) + \alpha f P(f), \qquad (1)$$

where $P(f)$ and $1 - P(f)$ are the fraction of failed and intact fibers, respectively, and the Young modulus E_f of intact fibers is taken to be unity $E_f = 1$. In Eq. (1) the first term provides the load carried by intact fibers while the second term is the load-bearing contribution of the failed ones. It can be seen that for the parameter setting $\alpha = 0$, the constitutive behavior of CDFBM Eq. (1) recovers the classical fiber bundle model where failed fibers do not carry any load [14–16, 20, 27].

It is important to note that Eq. (1) can be rewritten in the form

$$\sigma = (1 - \alpha) f \left[1 - P(f)\right] + \alpha f, \qquad (2)$$

which allows for an interesting alternative physical interpretation: when fibers are allowed to break only once but they retain their reduced Young modulus, the constitutive behavior of CDFBM is identical to another fiber bundle which is composed of two subsets of fibers with widely different strength characteristics but identical elastic behavior. A subset of αN fibers is unbreakable while the remaining $(1-\alpha)N$ fibers are breakable characterized by a threshold distribution P [21]. Very recently, we have demonstrated that the presence of unbreakable fibers results into a complex behavior of the system especially the avalanche statistics has substantial changes compared to the simple FBM [21]. These former results imply that in CDFBM an even richer behavior of the avalanche statistics can be expected which may provide a realistic description of certain materials.

For the general case, when fibers are allowed to fail k_{max} times and the fiber keep their final stiffness $\alpha^{k_{max}} E_f$ after having failed k_{max} times, the constitutive equation can be cast into the form

$$\sigma = f(1-P(f)) + \sum_{i=1}^{k_{max}-1} \alpha^i f \left[P(\alpha^{i-1}f) - P(\alpha^i f)\right] + \alpha^{k_{max}} f P(\alpha^{k_{max}-1} f) \qquad (3)$$

Throughout the paper the Weibull distribution

$$P(\sigma) = 1 - \exp\left[-\left(\sigma/\sigma_o\right)^m\right] \qquad (4)$$

is used for the breaking thresholds of fibers, where the values of the two parameters are fixed $m = 2$ and $\sigma_0 = 1$. The constitutive behavior Eq. (3) is illustrated in Fig. 1 and Fig. 2 for Weibull distributed failure thresholds Eq. (4). Note in the figures that the remaining load bearing capacity of fibers confers the material with elastic hardening. In fact, once all fibers have failed the constitutive curve $\sigma(f)$ converges to an asymptotic straight line and the system is characterized by an elastic constant $\alpha^{k_{max}} E_f$. As k_{max} increases, the asymptotic linear behavior of hardening is getting weaker and it is preceded by a longer and longer plateau. The larger k_{max} is, the flatter the constitutive curve becomes; in the limiting case of $k_{max} \to \infty$ the macroscopic material response becomes completely plastic. At a given value of k_{max} the shape of $\sigma(f)$ along the plateau regime can be controlled by the stiffness reduction parameter α. For low values of α, local maxima and minima can be observed. For a given k_{max} there exists always a critical value α_c of the stiffness reduction factor for which the wavy shape of Fig. 1 disappears, and in the parameter regime $\alpha > \alpha_c(k_{max})$ the plateau becomes monotonous and essentially flat. The critical value $\alpha_c(k_{max})$ and the shape of the constitutive curve $\sigma(f)$ in the vicinity of this critical point play an essential role in the statistics of bursts. Figure 2 presents the constitutive curves $\sigma(f)$ for different k_{max} at the corresponding critical value of α. It can be observed that the larger k_{max} is, the wider the plastic plateau turns.

The constitutive relation Eq. (3) can also be expressed as a relation between the applied load σ and the macroscopic deformation of the bundle f experienced by each

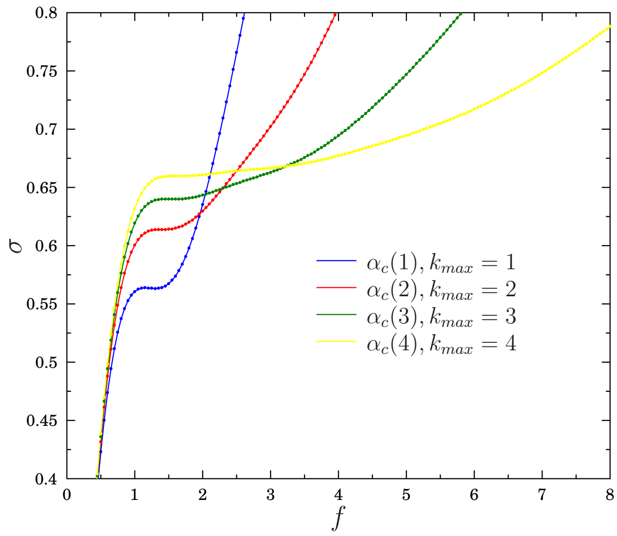

FIG. 2: Constitutive curves of CDFBM for different k_{max} at the corresponding critical value of the stiffness reduction factor α. As k_{max} increases the plastic plateau gets wider. The failure thresholds are Weibull distributed with the parameter values $m = 2$ and $\sigma_o = 1$.

fiber

$$\sigma = Y(f) f, \qquad (5)$$

where $Y(f)$ defines the effective Young modulus of the system at the deformation f

$$Y(f) = (1-P(f)) + \sum_{i=1}^{k_{max}-1} \alpha^i \left[P(\alpha^{i-1}f) - P(\alpha^i f)\right] + \alpha^{k_{max}} P(\alpha^{k_{max}-1} f) \qquad (6)$$

in units of E_f.

Quasi-static loading of the bundle can be carried out in such a way that the load is incremented until a single fiber breaks. Then the load of the broken fiber is overtaken by the remaining intact ones which might induce further breaking. The subsequent breaking and load redistribution steps can result in an entire avalanche of breakings. In order to understand the statistics of burst of breaking fibers, let us consider the case when a fiber which has broken j times until the deformation f was achieved, fails again. We have shown in Ref. [31] that the probability density function $p_j^{j+1}(f)$ of this event can be obtained in the form

$$p_j^{j+1}(f) = \alpha^j p(\alpha^j f). \qquad (7)$$

As a consequence, the Young modulus of the breaking fiber gets reduced which releases stress distributed among the fibers. This stress redistribution leads to an increase in the global deformation f which can be expressed as

$$\delta f_j = \frac{\alpha^j (1-\alpha) f}{Y(f)}, \quad (8)$$

where index j expresses that this strain increment appears as a consequence of a failure of fiber which has been broken j times before. Using Eqs. (7,8), the total probability that a fiber breaks as a consequence of a fiber breaking when the material is subject to a strain f reads as

$$p_{tot} = \sum_{j=0}^{k-1} \delta f_j p_j^{j+1}(f) = \frac{(1-\alpha)f}{Y(f)} \sum_{j=0}^{k-1} \alpha^{2j} p(\alpha^j f) \quad (9)$$

Using the expression for the Young modulus, and the fact that its derivative

$$\frac{dY(f)}{df} = (1-\alpha) \sum_{j=1}^{k-1} \alpha^{2j} p(\alpha^j f) \quad (10)$$

is closely related to the overall breaking probability $p_{tot}(f)$, we can express p_{tot} in the simple form

$$p_{tot}(f) = -\frac{fY'(f)}{Y(f)}. \quad (11)$$

Since the extrema of the constitutive curve satisfy $fY'(f) + Y(f) = 0$, in these points necessarily $p_{tot} = 1$ holds, which leads to the breaking of a macroscopic fraction of the sample, consistent with the $k_{max} = 1$ case studied in Ref. [21].

III. AVALANCHE DYNAMICS

Under a quasi-statically increasing external load, the damage and fracture of heterogeneous materials proceeds in a large number of steps of crack nucleation and sudden advancement of growing cracks. This process is accompanied by the release of elastic waves which can be recorded by the acoustic emission technique. The acoustic signals provide very valuable information about the microscopic dynamics of fracture of heterogeneous materials. In fiber bundle models, single fiber breakings can trigger an avalanche of breaking events which corresponds to the acoustic bursts of the experiments. One of the main advantages of FBMs is that they allow for the analytic derivation of the statistics of breaking bursts at least in the limit of global load sharing.

In the global load sharing limit of simple FBM, Hansen and Hemmer [15, 16] have proven that the probability density $D(\Delta)$ to observe an avalanche of size Δ, during a quasi-static loading process, has the form

$$\begin{aligned} D(\Delta) &= \frac{\Delta^{\Delta-1}}{\Delta!} \int_0^{f_m} p(f)(1-a_f) a_f^{\Delta-1} e^{-a_f \Delta} df \\ &\equiv \frac{\Delta^{\Delta-1}}{\Delta!} I(\Delta), \end{aligned} \quad (12)$$

where a_f is the average fraction of fibers which breaks as a result of an infinitesimal increase in the applied deformation f. For CDFBM a_f is identical to the total breaking probability $a_f = p_{tot}$ given by Eq. (11), which can further be simplified to the form

$$a_f = -\frac{d \ln Y(f)}{d \ln f}. \quad (13)$$

In the following we provide an analytic derivation of the burst size distribution of CDFBM starting from Eqs. (12, 13).

For convenience, we introduce the auxiliary function $I(\Delta)$ with the definition

$$I(\Delta) \equiv \int_0^{f_m} p(f) \frac{1-a_f}{a_f} e^{-\Delta[a_f - \ln a_f]} df. \quad (14)$$

We are interested in large burst events, and hence will concentrate on the region of large avalanches ($\Delta \gg 1$). In this regime the Stirling equation $\ln n! \simeq \left(n + \frac{1}{2}\right) \ln n - n + \ln \sqrt{2\pi}$ is used and the avalanche distribution $D(\Delta)$ can be expressed as

$$D(\Delta) \simeq \frac{e^{\Delta}}{\sqrt{2\pi} \Delta^{3/2}} I(\Delta). \quad (15)$$

Under global load sharing conditions, which is equivalent to the CDFBM with $k_{max} = 1$ and $\alpha = 0$, the upper integral limit in Eq. (14) is the location of the parabolic maximum of the constitutive curve f_m. Thus, for large Δ this integral is controlled by the maximum of the exponent in the integrand. The extreme condition of $\psi \equiv a_f - \ln a_f$ results in $\psi' = a_f'(1 - \frac{1}{a_f}) = 0$, according to a maximum at $a_f = 1$. Carrying out the Taylor expansions of a_f and ψ_f, it was shown in Refs. [15, 16] that the distribution $D(\Delta)$ simplifies to a power law

$$D(\Delta) \sim \Delta^{-\tau}, \quad (16)$$

with the exponent $\tau = 5/2$ for a broad class of disorder distributions, including the CDFBM with $k_{max} = 1$ and $\alpha = 0$, where the constitutive curve of the system has a single quadratic maximum [15, 16].

Even when the asymptotic behavior of the avalanche distribution is controlled by the extremum of ψ, there may exist situations where the macroscopic constitutive curve of the system has an inflexion point. This is the case if $\psi'' = 0$ at the maximum, a situation which happens whenever $a_f' = 0$ for $a_f = 1$. One then needs to continue the Taylor expansion of ψ to identify the relevant leading contribution. Following the usual procedure, one arrives at

$$I(\Delta) \simeq \frac{p(f_c) a''_{f_c} e^{-\Delta}}{2} \int_0^{\infty} df (f - f_c)^2 e^{\frac{3a''^2_{f_c}\Delta}{4!}(f-f_c)^4}. \quad (17)$$

which implies that the asymptotic decay of the avalanche size distribution is characterized by a different algebraic tail

$$D(\Delta) \simeq \frac{\Gamma\left(\frac{3}{4}\right)}{24\sqrt{3\pi a''_{f_c}}3^{1/4}}\Delta^{-9/4}. \quad (18)$$

Fig. 1 illustrates that such a scenario is found in the CDFBM with $k_{max} = 1$ when the stiffness reduction parameter α reaches its critical value $\alpha_c(1)$. As it has been discussed in Sec. II, for the maximum number of allowed breakings $k_{max} = 1$, at $\alpha = \alpha_c(1)$ the local quadratic maximum of the constitutive curve disappears, $\sigma(f)$ becomes monotonous and an inflection point is formed. The above analytic result Eq. (18) demonstrate that the presence of the inflexion point substantially changes the avalanche statistics of the system.

One can then generalize the analysis and consider a situation where the constitutive relation $\sigma(f)$ leads to an incremental average fiber breaking, a_f which gives rise to a generalized inflexion point of order n at the extremum of ψ of the location f_m. Carrying out again a Taylor expansion of ψ to leading order around its extremum, we arrive at

$$I(\Delta) \simeq \frac{p(f_c)a''_f e^{-\Delta}}{2}\int_0^{\infty} df(f-f_m)^n e^{\frac{(2n-1)a_f^{(n)^n}\Delta}{2n!}(f-f_m)^{2n}}, \quad (19)$$

where $a_{f_m}^{(n)}$ denotes the first non-vanishing derivative of a_f at f_m. It follows that the cumulative avalanche size distribution decays algebraically as

$$D(\Delta) \sim \Delta^{-\frac{4n+1}{2n}}. \quad (20)$$

This analytic result demonstrates that as the order of the inflexion point n increases, the size distribution of avalanches remains a power low but the exponent gradually decreases. In the limit of an infinitely large plastic plateau $n \to \infty$ the avalanche distribution will converge to $D(\Delta) \sim \Delta^{-2}$.

It is also interesting to analyze the statistics of avalanches around a prescribed neighborhood of a generalized local extremal point $(f_m; \sigma_m)$ of the constitutive curve of order n where $\frac{d^i\sigma}{df^i} = 0$ ($i = 1...n-1$ and $n \in Z$). Recently, it has been shown that restricting the analysis to the vicinity of the parabolic maximum of the constitutive curve, the avalanche size distribution shows a crossover between two power law regimes: the asymptotics of the distribution has an exponent 5/2 while the distribution of small avalanches decays slower with the exponent 3/2. Considering avalanches only at the maximum of $\sigma(f)$, a single power law remains with exponent 3/2 [17–20].

In the general case of a local extremal point $(f_m; \sigma_m)$ of order n, the size distribution of avalanches originating in the strain interval $f_0 \leq f \leq f_m$, can be cast into the form

$$D(\Delta, f_0) = \frac{\Delta^{\Delta-1}}{\Delta!}\int_{f_0}^{f_m} p(f)(1-a_f)a_f^{\Delta-1}e^{-a_f\Delta}df, \quad (21)$$

Hence, the asymptotics of the distribution reads as

$$D(\Delta, f_0) \sim \Delta^{-\frac{4n+1}{2n}}\left(\Gamma\left(\frac{3n+1}{2n}\right) - \Gamma\left(\frac{3n+1}{2n}, \frac{\Delta}{\Delta_c}\right)\right), \quad (22)$$

where the crossover avalanche size Δ_c scales with the strain interval as

$$\Delta_c \sim \frac{1}{(f_m - f_0)^{2n}}. \quad (23)$$

Depending on the avalanche size we can then identify two regimes in the avalanche size distribution

$$D(\Delta, f_0) \sim \begin{cases} \Delta^{-\frac{3}{2}} & \text{if } \Delta \ll \Delta_c \\ \Delta^{-\frac{4n+1}{2n}} & \text{if } \Delta \gg \Delta_c \end{cases} \quad (24)$$

When the avalanches are recorded in the vicinity of a generalized local extreme where $\frac{d^i\sigma}{df^i} = 0$ ($i = 1...n-1$ and $n \in Z$), we find that the power law has an exponent which also differs from the one characterizing the size distribution of all avalanches. This result generalizes previous findings reported in [17–20], where a constitutive behavior with a single parabolic maximum $n = 1$ was examined.

IV. COMPUTER SIMULATIONS

In order to obtain a deeper understanding of the microscopic breaking mechanism of CDFBM, we have developed a simulation technique and explored numerically the distribution of bursts of fiber failures in Ref. [31]. Under stress controlled loading conditions, the failure of each fiber is followed by a redistribution of load, which can induce further fiber breakings, resulting in an avalanche of failure events. Previously, we have analyzed numerically the avalanche statistics of the model varying the value of the number of failures k_{max} and of the stiffness reduction parameter α setting up an approximate phase diagram based on computer simulations [31]. In the following, based on the analytic results of Sections II and III, we deduce analytically the complete phase diagram of CDFBM on the $(\alpha; k_{max})$ plane classifying all possible functional forms of the burst size distributions. The analytic predictions are tested by computer simulations using a Weibull distribution of breaking thresholds Eq. (4) with the parameters $m = 2$ and $\sigma_0 = 1$. In the simulations the number of fibers is fixed $N = 160000$ and the bursts size distributions are averaged over two hundred samples.

It has been presented in Fig. 1, that after the initial elastic response, the constitutive curve of CDFBM displays a plateau regime, which can be non-monotonic; several local extrema and inflection points typically show up along the plateau. Varying the value of α and k_{max} the number and shape of the local extremal and inflexion points can be controlled. The above analytic calculations demonstrate that the presence of those local extreme values and their qualitatively different shape have

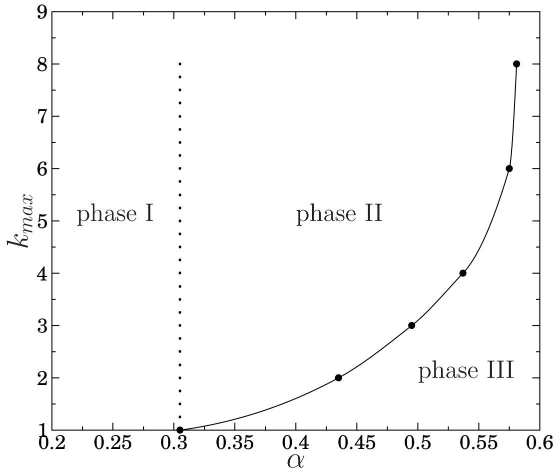

FIG. 3: Phase diagram of the continuous damage fiber bundle model characterizing the qualitatively different burst size distributions. The calculations of the phase boundaries were carried out analytically for Weibull distributed breaking thresholds with $\sigma_0 = 1$ and $m = 2$.

a substantial effect on the microscopic process of failure. Especially the asymptotics of the size distribution of breaking bursts is controlled by the mechanical response of the material near the local extrema and the last inflection point of the constitutive curves.

It is noticeable in Fig.1 that the local extreme of the constitutive curves of the CDFBM are not parabolic in general, i.e. the larger the value of k_{max} is, the flatter the peaks are. When fibers can fail only once $k_{max} = 1$, below the the critical stiffness reduction parameter $\alpha < \alpha_c(k_{max} = 1)$ the constitutive curve $\sigma(f)$ has a local maximum while above it $\sigma(f)$ becomes monotonous with an inflexion point. It can also be shown analytically that for $k_{max} > 1$ the constitutive curve has k_{max} local maxima, however, at the critical value $\alpha_c(k_{max} = 1)$ the last maximum turns into an inflexion point. This feature is illustrated in Fig.1. It follows that for any values of k_{max}, in the parameter regime $\alpha < \alpha_c(k_{max} = 1)$ the avalanche size distribution is controlled by the neighborhood of all maxima giving rise to an algebraic decay with an exponent 5/2. This scenario is represented by *Phase I* in the phase diagram of Fig. 3, where the burst distributions are described by Eq. (16) in agreement with Refs. [15, 16]. The critical point $\alpha_c(k_{max} = 1)$ can be determined analytically as $\alpha_c(1) = me^{-(1+m)/m}/\left[1 + me^{-(1+m)/m}\right]$. For the Weibull parameters $m = 2$ and $\sigma_0 = 1$ it has the value $\alpha_c(1) = 0.305$ which is represented by the dotted vertical line in the phase diagram Fig. 3.

It has been shown in Sec. III that for each k_{max} there exists a critical value of the stiffness reduction parameter $\alpha_c(k_{max})$ above which the constitutive curve becomes monotonous $d\sigma/df \geq 0$ (see Fig. 2). In this case the avalanche statistics is determined by a generalized singular point $(f_m; \sigma_m)$ of $\sigma(f)$ leading to a distinct behavior which is represented by *Phase III* in the phase diagram. The phase boundary in Fig. 3 separating *Phase II* and *Phase III* is the curve of $\alpha_c(k_{max})$ which can be determined as the minimum value of α for which $\frac{d\sigma}{df} = \frac{d^2\sigma}{df^2} = 0$ holds at a given k_{max}. In Section III we have proven analytically that when the constitutive curve does not present any local maximum, furthermore, a generalized singular point shows up, the size distribution of avalanches has a power law behavior with an exponent $D(\Delta) \sim \Delta^{-\frac{4n+1}{2n}}$. The value of n is directly related to the order of the first non vanishing derivative of the constitute curve $\frac{d^n\sigma(f)}{df^n} \neq 0$ at the generalized singular point $(f_m; \sigma_m)$. It is important to emphasize that due to the absence of local maxima of the constitutive curve $\sigma(f)$, in Phase III the avalanche size distribution has an asymptotic exponential decay characterized by a correlation length which diverges on approaching α_c from above. In order to numerically verify the analytic predictions on the burst size distribution and to analyze the diverging correlation length when approaching the line $\alpha_c(k_{max})$, we carried out computer simulations of CDFBM. The insets of Figs. 4(a) and 4(b) present the size distribution of bursts obtained by computer simulations for $k_{max} = 2$ and $k_{max} = 4$ in the parameter range $\alpha > \alpha_c(k_{max})$, i.e. inside *Phase III*. The corresponding critical values can be obtained as $\alpha_c(2) = 0.435$ and $\alpha_c(4) = 0.537$. It can be seen in the insets of Figs. 4(a, b) that in agreement with the analytic predictions, the cutoff of the avalanche size distributions $D(\Delta)$ rapidly increases when α approaches α_c from above.

To further analyze the effect of α varied inside Phase III, we introduce the scaling ansatz

$$D(\Delta) = \bar{\Delta}_{max}^{-\beta} g(\Delta/\overline{\Delta}_{max}^{\xi}) \qquad (25)$$

for the avalanche size distribution, $D(\Delta)$, obtained above the critical point $\alpha > \alpha_c(k_{max})$. In Eq. (25), the mean value of the maximum avalanche, $\overline{\Delta}_{max}$, is introduced as a scaling variable, while β and ξ are scaling exponents which must satisfy the relation $\beta = \tau\xi$. Figures 4(a) and 4(b) display the rescaled avalanche size distributions plotting $D(\Delta)\overline{\Delta}_{max}^{\beta}$ as a function of $\Delta/\overline{\Delta}_{max}^{\xi}$. The high quality data collapse obtained with the parameters $\beta = 3.12$ and $\xi = 1.4$ are consistent with a power law exponent $\tau = 2.23$. Additionally, in Fig. 4(b) the collapsed data corresponding to $k_{max} = 4$ and α values just above $\alpha_c(4)$ is consistent with $\beta = 3.28$ and $\xi = 1.6$, which correspond to a power law exponent $\tau = 2.05$. It is noticeable that the size of plastic plateau of the constitutive curve increases with increasing k_{max}. These values should be compared to the analytic predictions of 2.25 and 2.125 in the case of $k_{max} = 2$ and $k_{max} = 4$, respectively.

These results demonstrate that the exponent of the power law tends asymptotically to $\tau \to 2$ with increasing k_{max}. This scenario corresponds to a situation where

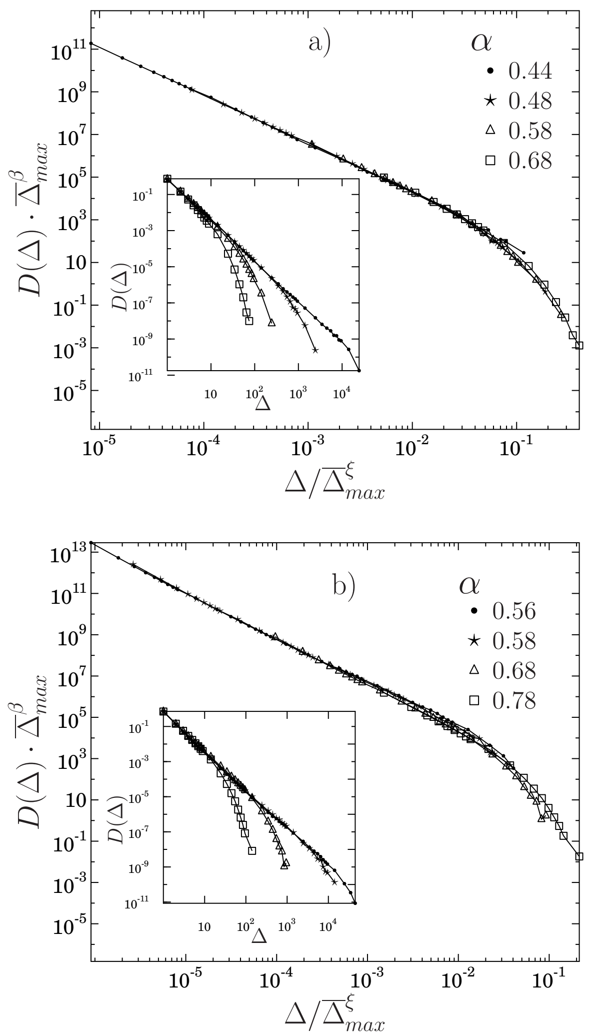

FIG. 4: The avalanche statistics obtained for a system with $k_{max} = 2$ (a) and $k_{max} = 4$ (b). Results for several values of α above $\alpha_c(k_{max})$ are shown. Rescaling the two axis according to the scaling formula Eq. (25), a very good quality data collapse is obtained. Non-normalized avalanche size distributions are presented in the insets.

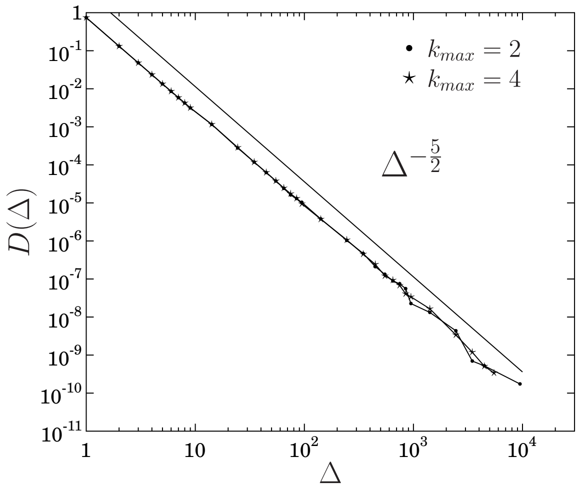

FIG. 5: Distribution of avalanches recorded from the beginning of the experiment till the first pick for $k_{max} = 2$ and $k_{max} = 4$. In both cases the value of α was chosen in the range $\alpha < \alpha_c(1)$.

the plastic plateau of the constitutive relation becomes flatter as k_{max} increases. According to the theoretical description of the previous section, the exponent Eq. (20) characterizing the asymptotic decay of the cumulative avalanche size distribution can vary between 5/2 when a local maximum controls the catastrophic avalanches, and 2 when the relevant region of the constitutive curve becomes sufficiently flat.

The fact that $\alpha_c(1) < \alpha < \alpha_c(k_{max})$ for $k_{max} > 1$ opens a region *phase II* in the phase plain, where the constitutive curve is non-monotonous, but where the first maximum is smaller than the subsequent ones. As a result, on increasing monotonously the applied stress the material explores the intermediate region where the material exhibits a non-trivial plastic behavior. The characteristic avalanche activity is located in the neighborhood of the consecutive maxima. We can probe this subsequent bursting activities by analyzing the avalanche size distribution for different strain windows along the constitutive curve. In Fig. 5 we show the corresponding avalanche distributions recorded till the first parabolic maximum, for two values of k_{max} displaying the generic algebraic decay $D(\Delta) \sim \Delta^{-\frac{5}{2}}$ with the usual mean field exponent 5/2. Under stress controlled loading the valleys of the constitutive curve (as displayed in Fig. 1, cannot be accessed and the right hand side of the different maxima does not contribute to the avalanche dynamics. However, we can analyze the avalanches which propagate in the system in the neighborhood of the different maxima from bellow. We observe in this case in Fig. 6 an algebraic avalanche distribution with exponent $-\frac{3}{2}$ independently of the shape of the maximum, as predicted from Eq. (22). Increasing α in phase II, the maxima subsequently disappear, but the contribution to the largest avalanches is provided by the last maximum of the constitutive curve. As we approach $\alpha_c(k_{max})$, the last remaining maximum merges with the increasing part of the constitutive relation associated to material hardening, and right at the critical value the maximum becomes a generalized inflection point.

V. DISCUSSION

We carried out a detailed study of the avalanche statistics of the continuous damage fiber bundle model where the fibers undergo a series of partial breaking events reducing gradually their stiffness. Slowly increasing the

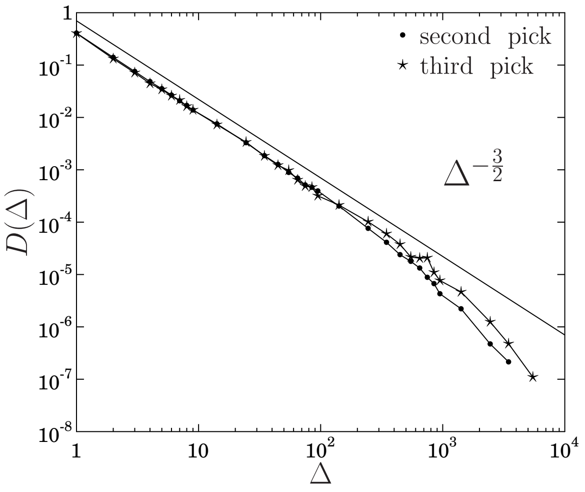

FIG. 6: Distribution of avalanches generated in the vicinity of intermediate peaks of the constitutive curve at the parameter values $k_{max} = 4$ and $\alpha = 0.40$.

external load on the bundle, fibers break in bursts due to the subsequent load redistribution over intact fibers. The model has two main parameters, i.e. the stiffness reduction factor and the total number of allowed failures. Varying these parameters, the model captures various types of materials' response which can have also experimental relevance.

As the main outcome of the work, we determined analytically the burst size distributions of the model and constructed a phase diagram of the system which characterizes all possible avalanche behaviors. We showed that the presence of macroscopic hardening and plastic behavior result in burst distributions different from the usual mean field result of FBM: power law functional forms arise with an exponent varying between 2.5 and 2.0 depending on the model parameters, which is then followed by an exponential cutoff. The analytic results are verified by extensive computer simulations.

Although we have focused in a family of FBM where analytic progress has been possible, the results obtained are more general and indicate the intricate behavior and richness of highly disordered materials which display a non-monotonous strain-load constitutive relation. The results obtained show that a careful understanding on the shape of the constitutive relation sheds light in the expected avalanche dynamics characterizing the failure process of materials on the micro-level.

Acknowledgment

This work is part of the Spanish-Hungarian Intergovernmental Scientific Project HH2005-0016. RCH acknowledges the financial support of the Spanish Minister of Education and Science, through a *Ramon y Cajal Program.* IP thanks CAICYT (FIS2005-01299) and DURSI (*Distinción de la Generalitat de Catalunya*) (Spain) for financial support. FK acknowledges the Janos Bolyai Fellowship of the Hungarian Academy of Sciences.

[1] *Statistical Models for the Fracture of Disordered Media.* Editors, H. J. Herrmann and S. Roux, North Holland (1990).
[2] *Statistical Physics of Fracture and Breakdown in Disordered Systems.* B. K. Chakrabarti and L. G. Benguigui, Clarendon Press, Oxford (1997).
[3] M. J. Alava, P. K. V. V. Nukala, and S. Zapperi *Adv. Phys.* **55**, 349 (2006).
[4] A. Petri, G. Paparo, A. Vespignani, A. Alippi, and M. Costantini, Phys. Rev. Lett. **73**, 3423 (1994).
[5] A. Garcimartín, A. Guarino, L. Bellon, and S. Ciliberto, Phys. Rev. Lett. **79**, 3202 (1997).
[6] A. Guarino, A. Garcimartín, and S. Ciliberto, Eur. Phys. J. B **6**, 13 (1998).
[7] L. I. Salminen, A. I. Tolvanen, and M. J. Alava, Phys. Rev. Lett. **89**, 185503 (2002).
[8] S. Deschanel1, L. Vanel, G. Vigier, N. Godin and S. Ciliberto, Int. J. Fract. **140**, 87 (2006).
[9] S. Deschanel, L. Vanel, N. Godin, and S. Ciliberto, J. Stat. Mech. P01018 (2009).
[10] D. Bonamy, S. Santucci, and L. Ponson, Phys. Rev. Lett. **101**, 045501 (2008).
[11] H. Nechad, A. Helmstetter, R. El Guerjouma, and D. Sornette, Phys. Rev. Lett. **94**, 045501 (2005).
[12] M. B. J. Meinders and T. van Vliet, Phys. Rev. E **77**, 036116 (2008).
[13] M. R'Mili, M. Moevus, and N. Godin, Composites Science and Technology **68**, 1800 (2008).
[14] H. E. Daniels, Proc. R. Soc. London A **183**, 405 (1945).
[15] A. Hansen and P. C. Hemmer, Phys. Lett. A **184**, 394 (1994).
[16] M. Kloster, A. Hansen, and P. C. emmer, Phys. Rev. E **56**, 2615 (1997).
[17] S. Pradhan and B. K. Chakrabarti, Phys. Rev. E **65**, 016113 2002.
[18] S. Pradhan, A. Hansen, and P. C. Hemmer, Phys. Rev. E **74**, 016122 (2006).
[19] S. Pradhan and A. Hansen, Phys. Rev. E **72**, 026111 (2005).
[20] S. Pradhan, A. Hansen, and P. C. Hemmer, Phys. Rev. Lett. **95**, 125501 (2005).
[21] R. C. Hidalgo, K. Kovacs, I. Pagonabarraga, and F. Kun, Europhys. Lett. **81**, 54005 (2008).
[22] T. Baxevanis and T. Katsaounis, Phys. Rev. E **75**, 046104 (2007).
[23] F. Raischel, F. Kun, and H. J. Herrmann, Phys. Rev. E **74**, 035104(R) (2006).
[24] F. Raischel, F. Kun, and H. J. Herrmann, Phys. Rev. E **77**, 046102 (2008).
[25] U. Divakaran and A. Dutta, Phys. Rev. E **75**, 011117

(2007).
[26] U. Divakaran and A. Dutta, Phys. Rev. E **75**, 011109 (2007).
[27] R. C. Hidalgo, Y. Moreno, F. Kun, and H. J. Herrmann, Phys. Rev. E **65**, 46148 (2002).
[28] R. C. Hidalgo, S. Zapperi, and H. J. Herrmann, J. Stat. Mech. P01004 (2008).
[29] S. Zapperi, A. Vespignani, and H. E. Stanley, Nature **388**, 658 (1997).
[30] F. Kun, S. Zapperi, and H. J. Herrmann, Euro. Phys. J. B **17**, 269 (2000).
[31] R. C. Hidalgo, F. Kun, and H. J. Herrmann, Phys. Rev. E **64**, 066122 (2001).